Autonomous Vehicle Logistic System: Joint Routing and Charging Strategy

James J. Q. Yu, *Member, IEEE*, and Albert Y. S. Lam, *Senior Member, IEEE*

***Abstract*— The smart city embraces gradual adoption of autonomous vehicles (AVs) into the intelligent transportation system. Contributed by their full-fledged controllability, AVs can respond to instantaneous situations with high efficiency and flexibility. In this paper, we propose a novel AV logistic system (AVLS) to accommodate logistic demands for smart cities. We focus on determining the optimal routes for the governed AVs in consideration of various requirements imposed by the vehicles, logistic requests, renewable generations, and the underlying transportation system. By coordinating their routes and charging schedules, the system can effectively utilize the renewable energy generated by distributed generations. We formulate the joint routing and charging problem in the form of quadratic-constrained mixed integer linear program. To improve its scalability, we develop a distributed solution method via dual decomposition. We conduct extensive simulations to evaluate the performance of proposed system and solution methods. The results show that AVLS can effectively utilize excessive renewable energy while accomplishing all logistic requests. The distributed solution can develop near-optimal solutions with compelling improvement in computational speed.**

***Index Terms*— Autonomous vehicle, logistics system, vehicle routing, vehicle charging, smart city.**

I. Introduction

With increasing awareness of environmental protection, the public is embracing the green revolution of adopting energy-efficient and clean technologies [1]. Among the promising technologies constructing the future sustainable smart cities, the intelligent transportation system (ITS) is one of the essential components. It is envisioned that ITS can help accommodate a massive volume of transportation demand while exerting limited and controllable damage to the environment [2]. By upgrading the transport carriers and backend supporting management systems, ITS can support higher transportation capacity and provide a safer travel environment to the citizens.

Recent industrial investigations reveal that the autonomous vehicles (AV) will revolutionize the automobile industry and transportation systems, and become prevalent in the next decade [3], [4]. AVs are well-known for their capabilities to adapt to real-time traffic conditions and to determine optimal driving patterns. These features benefit the transportation system in many ways, such as less traffic collisions and greater transportation throughput. Moreover, AVs are typically connected and online-controllable, which means that real-time driving instructions can be remotely issued by a specific control center [5]. In this way, the control center can collectively manage and optimize the routes of a fleet of AVs to achieve certain social objectives, such as reducing traffic congestion.

In addition, one important function of ITS is to handle the so-called "last-mile" delivery, which refers to the process of conveying goods from transportation hubs to final destinations in supply chain management [6]. The increasing demand of last-mile delivery operations advocates the adoption of a more energy-efficient and environmentally acceptable form of city logistics [7]. In fact, AV can act as a good candidate to fulfill these requirements. With the adoption of AVs in the modern transportation system, they can be employed to construct a new logistic system with high efficiency, flexibility, and capacity.

It is also believed that the future sustainable smart city will incorporate lots of renewable generations into the power grid. However, the volatility and intermittency of renewables bring great challenges to the power system stability [8]. One possible solution is to utilize the batteries of electric vehicles (EVs) to mitigate the fluctuation of renewable generations [9], [10]. Since most AVs are made in the form of EVs and it is much easier to manipulate the driving schedules of AVs collectively, we believe AVs can greatly contribute to the sustainability of future smart cities and human society.

In this paper, we propose the Autonomous Vehicle Logistic System (AVLS) to provide smart city logistic services. AVLS aims to integrate AVs, logistics, and the renewable generation into one system. It manages a fleet of AVs to accommodate logistic requests. We focus on investigating how to provide the optimal routes for all AVs in AVLS to serve their logistic requests. In the meantime, the routes can strategically guide the vehicles to get charged at appropriate locations with distributed generations (DGs). This helps utilize the excessive energy at DGs, which otherwise have to be curtailed or injected into the main grid, which may lead to potential stability issues [11]. The contribution of this paper is summarized as follows:

- We propose AVLS for logistic services with AVs, which can also help mitigate the renewable generation fluctuations of distributed generations and improve renewable penetration;

Manuscript received May 17, 2017; revised September 1, 2017; accepted October 19, 2017. Date of publication November 20, 2017; date of current version June 28, 2018. This work was supported by the National Natural Science Foundation of China under Grant 51707170. The Associate Editor for this paper was S. Djahel. *(Corresponding author: Albert Y. S. Lam.)*

The authors are with the Department of Electrical and Electronic Engineering, The University of Hong Kong, Hong Kong (e-mail: jqyu@eee.hku.hk; ayslam@eee.hku.hk).

Color versions of one or more of the figures in this paper are available online at http://ieeexplore.ieee.org.

Digital Object Identifier 10.1109/TITS.2017.2766682

- We formulate the joint routing and charging problem to determine the optimal AV routes based on some social objectives;
- We design a distributed method to efficiently solve the proposed optimization problem;
- We validate the performance of AVLS with extensive simulations.

The rest of this paper is organized as follows. We provide the background of this work in Section II. Then we elaborate the system model of AVLS in Section III, including its essential system components and the operational design. Section IV formulates the joint routing and charging problem for AVLS, and Section V discusses a distributed solution to the problem. In Section VI, the system performance is evaluated with comprehensive simulations. Finally, we conclude this paper in Section VII.

II. Background

AVs and renewable generations are among the essential components of the future smart city. Some previous work investigated the driving behavior of AVs, the interaction of AVs, and the integration of AVs with renewable generations. For instance, [12] introduced a local path planner to compute the AV driving trajectories and [13] investigated the trajectory control design for autonomous driving. In addition, cooperative AV transportation pattern has also attracted lots of attention. Reference [14] analyzed the coupling of AV control, communication, and sensing in multi-vehicle systems for a safer, efficient, and sustainable road transportation. Reference [15] devised a decentralized cooperative lane-changing decision-making algorithm for AVs to improve stability, efficiency, homogeneity, and safety.

AVs are typically electric energy driven and they contain batteries to store energy for propulsion. Hence, as EVs, AVs can actively participate in vehicle-to-grid (V2G) systems to support power system services. While there are few existing results on AVs participating in V2G (e.g., [16]), a plethora of literature is devoted to studying EV-V2G systems. EVs are shown to be effective to provide services like demand response [17]–[19] and ancillary services [20]–[22]. Through coordinated charging operations, the profits of EV owners and/or system operators can be improved [10], [23]. All these suggest that EVs can benefit the power system operation and the adoption of EVs to the modern transportation system is encouraged, and so as AVs.

Moreover, the gradual adoption of AVs and EVs advocates their active participation in logistic services. These "green" vehicles are expected to significantly improve the environment-friendliness of modern logistic systems. For example, [24] showed that a large scale AV/EV-driven logistic system is becoming more feasible. EVs have demonstrated advantages over the traditional diesel-driven counterpart in real-world implementations in China [25] and Portugal [26]. To the best of our knowledge, there is no existing research on vehicle-charging logistic systems. We aim to bridge this research gap in this paper.

AVLS can be considered as a variant of the AV public transportation system (AVPTS) [27], which utilizes AVs for public transportation. In this system, a control center manages a fleet of AVs and coordinates their driving schedules to provide public transportation services. [27] investigated the admission control and scheduling while [28] and [29] studied its pricing mechanisms. While AVLS shares some design principles with AVPTS, AVPTS cannot be adopted for the logistic needs directly. For instance, logistic requests typically have arrival deadlines, which are not considered explicitly in AVPTS. In addition, AVPTS does not include a vehicle charging scheme and thus how it can integrate with smart grid is still unknown. In this work, based on AVPTS, we design AVLS which is tailored for logistics and can be integrated with the smart grid.

III. System Model

This section focuses on the architecture of AVLS. We first introduce the building blocks of the system and then its operations.

A. System Components

The symbols used in this work are summarized in Table I.

1) Transportation Network: AVs traverse in the transportation network for logistic purposes. The network is modeled by a directed graph $\mathrm{G}(\mathcal{V}, \mathcal{E})$. Each edge $(i, j) \in \mathcal{E}$ is associated with a distance D_{ij} (km) indicating the travel distance from i to j, and traffic speed S_{ij} (km/h), which describes the average speed of traffic flow from i to j at time t. Note that D_{ij} and S_{ij} can be different from D_{ji} and S_{ji} to account for the possible asymmetry of roads. From D_{ij} and S_{ij}, we can also determine the corresponding travel time L_{ij}.

2) Autonomous Vehicles: We denote the set of AVs in AVLS by $\mathcal{K}$. We consider heterogeneous settings such that the AVs can be of different types or have different properties. Each $k \in \mathcal{K}$ can be represented by a tuple $\langle \underline{P}_k, \overline{P}_k, B_k, \eta_k, C_k, \mathcal{R}_k^-, R_k^+, \overline{T}_k, \mathcal{Q}_k \rangle$, where $\underline{P}_k$ is the starting location of k, $\overline{P}_k$ is its final destination of k after all deliveries, B_k is its battery capacity (kWh), η_k is its charging efficiency (%), C_k is the initial state-of-charge (SOC, %), $\mathcal{R}_k^-$ equals $\{R_k^{ij-}, \forall\, (i, j)\}$ where R_k^{ij-} (kWh/km) is its energy consumption rate when driving on (i, j), R_k^+ is its charging rate (kW), $\overline{T}_k$ is the deadline for k to arrive at $\overline{P}_k$, and $\mathcal{Q}_k$ is the set of logistic requests previously assigned to k.

3) Logistic Requests: We consider a collection of logistic requests for goods delivery. Each request q is specified by a tuple $\langle P'_q, \underline{T}'_q, \overline{T}'_q, D'_q \rangle$, where P'_q is the delivery location of q, $\underline{T}'_q$ and $\overline{T}'_q$ ($\underline{T}'_q < \overline{T}'_q$) are the earliest and latest delivery times, respectively. Disembarking the goods at P'_q incurs service time D'_q.

4) Renewable Distributed Generations: We follow [30] and [31] to model DGs in AVLS. We consider a set of grid-connected renewable DGs[1] $g \in \mathcal{G}$ in AVLS, each of which locates at $v_g \in \mathcal{V}$. While DGs generate energy from the renewables to support their local consumptions, any excessive energy can also be used to charge the AVs. We consider DG g providing at most $\omega_g(t) \geq 0$ (kW) power to charge its

[1]The model can also represent the conventional DGs which utilize dispatchable energy sources.

TABLE I
SUMMARY OF DEFINED SYMBOLS

Transportation Network Model		**Autonomous Vehicle Model**	
$\mathcal{V}$	Set of road intersections, charging stations, and logistic service points.	$\mathcal{K}$	Set of AVs in the system.
v, i, j	Nodes in $\mathcal{V}$.	k	An AV in $\mathcal{K}$.
$\mathcal{E}$	Set of road segments connecting $\mathcal{V}$.	$\underline{P}_k$, $\overline{P}_k$	Starting and final location of k.
(i,j)	An edge in $\mathcal{E}$ starting from i to j.	B_k, η_k	Battery capacity and charging efficiency of k.
D_{ij}	Distance of (i,j).	C_k	Initial SOC of k (%).
S_{ij}, L_{ij}	Average traffic speed and travel time of (i,j).	$\mathcal{R}_k$	Set of energy consumption rates of k.
Logistic Request Model		R_k^{ij-}, R_k^{+}	Energy consumption rate on (i,j) in kWh/km, and charging rate (kW) of k.
q	A logistic request.	$\overline{T}_k$	Deadline of k to arrive its final location.
P'_q	The delivery location of q.	$\mathcal{Q}_k$	Set of logistic requests served by k.
$\underline{T}'_q$, $\overline{T}'_q$	The earliest and latest delivery times of q.	**Renewable Distributed Generation Model**	
D'_q	The service time of q at its delivery location.	$\mathcal{G}$	Set of renewable DGs in the system.
Depot Model		g	A renewable DG in $\mathcal{G}$.
$\mathcal{D}$	Set of all depots in the system.	v_g	The location of g.
d	A depot in $\mathcal{D}$.	$\omega_g(t)$	The excessive charging power of g at time t in kW.
v_d	The location of d.		

Optimization Variables		**Problem Transformation Variables (Section IV-D)**	
x_{ij}^k	Binary variable representing if k traverses (i,j).	$\mathbb{T}$	The discretized time horizon.
t_j^k	The time when k arrives at j.	τ, $\overline{\tau}$	An arbitrary time slot in $\mathbb{T}$ and total time slots.
d_j^k	The duration of stay at j for k.	Δ_t	Duration of a time slot.
ε_j^k	The amount of energy charged at j for k.	$u_j^k(\tau)$	Binary indicator on if AV k charges at j in τ.
c_j^k	SOC of k at j.	$p_j^k(\tau)$	Averaged $\rho_j^k(t)$ during τ.
$\rho_j^k(t)$	Charging profile function of k at j over t.	$\overline{\omega}_g(\tau)$	Power supply of g at τ: $\int_{\tau\Delta_t}^{(\tau+1)\Delta_t} \omega_g(t)dt/\Delta_t$.
Distributed Solution Variables (Section V)			
λ_g^τ	Lagrangian multiplier.	Z_{P}	The optimal objective value of (19) for all possible Λ.
Θ_g	Shorthand for $\sum_{\tau\in\mathbb{T}} \lambda_g^\tau p_{v_g}^k(\tau)$.	$Z(\Lambda)$	The optimal objective value of (19) for a given Λ.
Ω	Shorthand for $\sum_{g\in\mathcal{G}}\sum_{\tau\in\mathbb{T}} \lambda_g^\tau \omega_g(\tau)$.	$p_{v_g}^{k*}(\tau,i)$	The optimal value of $p_{v_g}^k(\tau)$ in Problem 3 at the i-th iteration.
Λ	Set of Lagrangian multipliers $\{\lambda_g^\tau \vert g\in\mathcal{G},\tau\in\mathbb{T}\}$.	$\lambda_g^\tau(i)$	The value of λ_g^τ at the i-th iteration.
$\mathcal{X}'$	Solution space of Problem 1 except (17a).		
$G_k^*(\delta,\Lambda)$	The optimal value of Problem 3.		
$\alpha_g^\tau(i)$	The step size for sub-gradient solution.		

associated AVs with its excessive energy at time t. As DGs can serve as a platform for AVs to participate in V2G, $\omega_g(t)$ represents the charging power requested for V2G at g at time t, which is similar to the implementation discussed in [16].

5) Depots: Depots refer to those places where goods are loaded to the vehicles [32]. We consider a set of depots $d \in \mathcal{D}$, which is located at $v_d \in \mathcal{V}$. In AVLS, the depots can also be used to charge the vehicles. While DGs are scattered in the city, returning to the depots for charging may be time-consuming and cost-ineffective. Therefore, how to optimally route AVs to deliver goods while charging at nearest DGs or depots is an important problem.

B. System Operations

As AVPTS [27], we consider a control center which instructs its governed AVs how to route and get charged in the transportation network based on certain goods delivery requirements. The complete delivery process can be divided into two phases: planning and implementation. In the former, the control center determines the routing and charging plan for AVs as follows. Each AV is assumed to be initially parked at a certain depot, where the goods to be delivered are stored. Goods are loaded to the vehicles based on the methods described in [33] and [34]. Then the control center gathers the required information about the transportation network, AVs, and logistic requests. At this time, the participating DGs also report to the system their estimated excessive energy, which can be used to charge the AVs [35]. Next it determines the routing and charging plans for the AVs with the considerations of the logistic requests and real-time traffic conditions. Finally the AVs carry out the plans for implementation. Sometimes during the implementation, information, such as traffic speeds and DG energy predictions, needs to be updated in real-time. In such cases, the control center can re-determine the routing and charging plan based on the new information.

In the system, the control center needs to actively collect traffic and vehicular information from time to time. Thanks to the development of various vehicular communication technologies, the data collection process can be facilitated by a certain wireless vehicular communication system. For instance, IEEE 802.11p [36] defines the standard for wireless vehicular communications to support intelligent transportation system applications. Vehicular ad hoc networks (VANET) can be set up to accommodate the wireless communication demand [37]. In addition, in the proposed system, the control instructions and the required data are not unremitting. Specifically, the driving plan can be sent to the vehicles for a short period of time and then only occasional connectivity is required for subsequent positioning and data collection. Hence, continuous connectivity is not necessary in the system, and VANET can be used to facilitate the transmission [37].

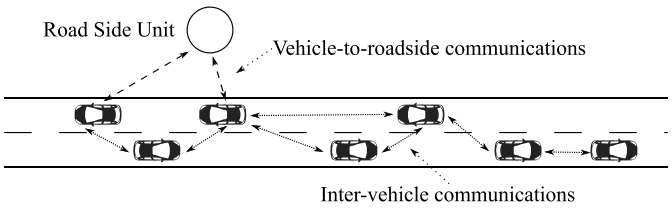

Fig. 1. A simplified model of VANET.

Fig. 1 illustrates how VANET constructs and functions. The communication network is facilitated by both vehicle-to-roadside base station communications and inter-vehicle communications. The technology employs the moving vehicles as wireless routers or nodes to constitute a ad-hoc wireless communication network with vehicles [37].

In AVLS, since the deadlines for delivery are fixed, a fast planning phase allows us to reserve more time for the actual implementation. As previously introduced, the planning phase is composed of three steps: information gathering, vehicle allocation, and optimization. With advanced vehicular communications, the data collection and route assignment can be done in seconds. In addition, the process of allocating goods to different vehicles can also be accomplished very fast [34]. Hence, it is essential to develop a fast and scalable strategy to determine the routing and charging plan. The relationship between system size and computational time will be investigated in Section VI-B.

IV. AVLS Routing and Charging Optimization

As discussed in Section III, one key problem in AVLS is to develop the optimal routing and charging plans for all participating vehicles. In this section, we formulate the joint routing and charging optimization problem.

A. Decision Variables

We define a binary variable x_{ij}^k to indicate which roads AV k should traverse, as follows:

$$x_{ij}^k = \begin{cases} 1 & \text{if } k \text{ traverses } (i,j) \in \mathcal{E} \\ 0 & \text{otherwise} \end{cases} \quad \forall k \in \mathcal{K}, \forall i, j \in \mathcal{V}.$$

For the ease of formulation, we assume that an AV can visit each node in the graph at most once[2]. We also describe the status of AV k at road intersection $j \in \mathcal{V}$ with the following:

- $t_j^k \geq 0$: The time when k arrives at j;
- $d_j^k \geq 0$: The duration of stay at j for k;
- $\varepsilon_j^k \geq 0$: The amount of energy charged at j for k;
- $0 \leq c_j^k \leq 1$: SOC of k at j;
- $\rho_j^k(t) \geq 0$: Charging profile function of k at j, which describes the charging power of the vehicle at the intersection and time t.

If k will not visit j, the corresponding variables and function above can be ignored.

B. Objective Functions

In this paper, we consider three different practical objectives for the joint routing and charging problem:

[2]In practice, we can create multiple nodes for the same location if it needs to be visited for multiple times.

1) Total Driving Distance: The total driving distance is a key concern when we decide the routes of vehicles [38], [39]. Since longer traveling distance imply more energy consumption and heavier traffic, shorter routes are more preferable. Thus we get

$$\text{minimize } D = \sum_{k \in \mathcal{K}} \sum_{(i,j) \in \mathcal{E}} D_{ij} x_{ij}^k. \tag{1}$$

2) Charged DG Energy: Most DGs are powered by the renewables. We will further enhance renewable penetrations if we can efficiently utilize the excessive energy generated. In this case, we can charge the vehicles with the excessive energy. This can be achieved with the following objective function:

$$\text{maximize } P = \sum_{k \in \mathcal{K}} \sum_{g \in \mathcal{G}} \varepsilon_{v_g}^k. \tag{2}$$

3) Delivery Time: For a logistic system, we aim to deliver the goods as earliest as possible and we have

$$\text{minimize } T = \sum_{k \in \mathcal{K}} t_{\overline{P}_k}^k, \tag{3}$$

which minimizes the total amount of time required for AVs to reach their final destinations $\overline{P}_k$ after delivering all goods on-board.

C. Constraints

1) Route Constraints: In AVLS, each AV is pre-allocated with some logistic request(s) based on those methods described in [33] and [34]. A vehicle should reach the corresponding destinations of the assigned requests for delivery. This can be ensured by having

$$\sum_{i \in \mathcal{V}} x_{ij}^k \geq 1, \quad \forall k \in \mathcal{K}, \forall j \in \{P_q' | q \in \mathcal{Q}_k\}. \tag{4}$$

It means that k should take at least one road that leads to the destinations of the assigned requests.

We model vehicular routes with the network flow model. The route for k is composed of multiple consecutive roads, and the connectivity is guaranteed by:

$$\sum_{i \in \mathcal{V}} x_{ij}^k - \sum_{i \in \mathcal{V}} x_{ji}^k = \begin{cases} 0 & \forall k \in \mathcal{K}, \forall j \in \mathcal{V} \setminus \{\underline{P}_k, \overline{P}_k\} \\ 0 & \forall k \in \mathcal{K}, \forall j \in \mathcal{V}, \underline{P}_k = \overline{P}_k \\ -1 & \forall k \in \mathcal{K}, j = \underline{P}_k, \underline{P}_k \neq \overline{P}_k \\ 1 & \forall k \in \mathcal{K}, j = \overline{P}_k, \underline{P}_k \neq \overline{P}_k, \end{cases} \tag{5}$$

where $\sum_{i \in \mathcal{V}} x_{ij}^k$ and $\sum_{i \in \mathcal{V}} x_{ji}^k$ are the incoming and outgoing flows of j, respectively. In (5), the first case ensures that for all road intersections other than a source or destination of k, if k reaches j from a road, an incoming flow will lead to an outgoing one. The remaining cases confirm that if the source and destination are different, there should be an outgoing flow and an incoming flow at the source and destination, respectively. Otherwise, the number of incoming and outgoing flows should be the same. Hence, (5) guarantees that the routes are connected.

2) Time Constraints: Recall that d_j^k defines the duration of stay at j for k. During the stay, Vehicle k can get charged from the DG and unload the goods if needed. If so, the stay should be at least long enough to unload the necessary goods, i.e.,

$$d_j^k \geq D'_q, \quad \forall k \in \mathcal{K}, \ \forall j \in \{P'_q | q \in \mathcal{Q}_k\}. \tag{6}$$

Moreover, traversing the roads take time. When k passes through (i, j), t_j^k should be no less than t_i^k with d_i^k and the travel time on (i, j). Hence we have:

$$t_j^k \geq t_i^k + d_i^k + L_{ij}, \quad \forall k \in \mathcal{K}, \forall i \in \mathcal{V}, \forall j \in \mathcal{V} \setminus \underline{P}_k, \forall x_{ij}^k = 1. \tag{7}$$

Moreover, the goods should arrive at their destinations within the expected earliest and latest times, i.e.,

$$\underline{T}'_q \leq t_j^k \leq \overline{T}'_q, \quad \forall k \in \mathcal{K}, \ \forall q \in \mathcal{Q}_k, j = P'_q. \tag{8}$$

Finally, the deadline $\overline{T}_k$ for k to arrive at its destination $\overline{P}_k$ should be caught:

$$t_{\overline{P}_k}^k \leq \overline{T}_k, \forall k \in \mathcal{K}. \tag{9}$$

3) Charging Constraints: The amount of energy charged by k at j is limited by its duration of stay, which gives:

$$\varepsilon_j^k \leq d_j^k R_k^+, \quad \forall k \in \mathcal{K}, \forall j \in \{v_g | g \in \mathcal{G}\} \cup \{v_d | d \in \mathcal{D}\}, \tag{10a}$$

$$\varepsilon_j^k = 0, \quad \forall k \in \mathcal{K}, \forall j \notin \{v_g | g \in \mathcal{G}\} \cup \{v_d | d \in \mathcal{D}\}. \tag{10b}$$

Constraint (10a) guarantees that the amount of energy charged at the DGs and depots must not exceed the maximum possible amount, which is achieved by charging at full rate R_k^+ during the stay. For those intersections without charging capability, no charging is possible, which is described by (10b).

Moreover, SOC should be updated according to the driving consumption and charging conditions. If k drives through (i, j), based on the SOC at i, the SOC at j can be computed by removing the energy spent on (i, j), and adding the charged energy at j. Hence we have:

$$c_j^k = c_i^k + \frac{\varepsilon_i^k - D_{ij} R_k^{ij-}}{B_k}, \quad \forall k \in \mathcal{K}, \ \forall i \in \mathcal{V}, \ \forall j \in \mathcal{V} \setminus \underline{P}_k, \ \forall x_{ij}^k = 1, \tag{11a}$$

$$c_j^k = C_k, \quad \forall k \in \mathcal{K}, \ \forall i \in \mathcal{V}, j = \underline{P}_k. \tag{11b}$$

4) DG Constraints: DG g provides power for charging at $\omega_g(t)$, which can be used to serve all those AVs stationed at g at time t. Hence we have

$$\sum_{k \in \mathcal{K}} \rho_{v_g}^k(t) \leq \omega_g(t), \quad \forall g \in \mathcal{G}, \ \forall t \geq 0. \tag{12}$$

To convert power into energy, we have

$$\varepsilon_j^k = \int_{t_j^k}^{t_j^k + d_j^k} \eta_k \rho_j^k(t) dt, \quad \forall k \in \mathcal{K}, \ \forall j \in \mathcal{V}. \tag{13}$$

The charging power is also limited by the maximum charging rate of k:

$$\rho_j^k(t) \leq R_k^+, \quad \forall k \in \mathcal{K}, \ \forall j \in \mathcal{V}, \ \forall t \geq 0. \tag{14}$$

D. Linear Transformation and Function Constraint Handling

We can see that all the objective functions and most constraints are affine, which are relatively easy to be handled. However, constraints (7) and (11a) are conditioned on $x_{ij}^k = 1$, which cannot be directly modeled without prior knowledge of x_{ij}^k. Moreover, (12)–(14) are based on $\rho_j^k(t)$, which cannot be effectively addressed by most optimization solvers, e.g., [40]. In this section we propose practical solutions to handle these issues. We first transform (7) into an equivalent linear form. We consider the following two cases:

- When x_{ij}^k is zero, AV k will not visit j from i along road (i, j). So there is no clear relation between t_i^k and t_j^k. t_j^k is only confined by its feasible range, i.e., $[0, +\infty)$;
- When x_{ij}^k is one, t_j^k must be greater than or equal to RHS of (7).

Hence, we can transform (7) into the following linear inequality:

$$t_j^k \geq t_i^k + d_i^k + L_{ij} - M(1 - x_{ij}^k), \quad \forall k \in \mathcal{K}, \forall i \in \mathcal{V}, \forall j \in \mathcal{V} \setminus \underline{P}_k, \tag{15}$$

where M is a sufficiently large number.

Similarly, (11a) can be recast as

$$c_j^k \leq c_i^k + (\varepsilon_i^k - D_{ij} R_k^{ij-})/B_k + M(1 - x_{ij}^k), \tag{16a}$$

$$c_j^k \geq c_i^k + (\varepsilon_i^k - D_{ij} R_k^{ij-})/B_k - M(1 - x_{ij}^k), \quad \forall k \in \mathcal{K}, \forall i \in \mathcal{V}, \forall j \in \mathcal{V} \setminus \underline{P}_k. \tag{16b}$$

When x_{ij}^k is one, (16) is equivalent to (11a). Meanwhile, when x_{ij}^k is zero, c_j^k has no clear relation with c_i^k as k does not take road (i, j). In such cases, RHS of (16a) is greater than one, and RHS of (16b) is smaller than zero. Considering $0 \leq c_j^k \leq 1$, (16) does not confine the value of c_j^k when $x_{ij}^k = 0$.

Finally we address the constraints that involve function $\rho_j^k(t)$, namely, constraints (12)–(14). We approximate those constraints by discretizing the time horizon into a number of time slots. To do this, additional ancillary variables are required, which are defined as follows:

- $\mathbb{T}$: The discretized time horizon;
- $\overline{\tau}$: Total number of time slots;
- τ: A time slot in $\mathbb{T}$;
- Δ_t: Duration of a time slot;
- $u_j^k(\tau) \in \{0, 1\}$: Binary indicator on if AV k is charging at j in time slot τ;
- $p_j^k(\tau)$: Averaged $\rho_j^k(t)$ during τ;
- $\overline{\omega}_g(\tau) = \int_{\tau \Delta_t}^{(\tau+1)\Delta_t} \omega_g(t) dt / \Delta_t$: Power supply of g at τ.

Hence, (12)–(14) can be respectively transformed into:

$$\sum_{k \in \mathcal{K}} p_{v_g}^k(\tau) \leq \overline{\omega}_g(\tau), \quad \forall g \in \mathcal{G}, \forall \tau \in \mathbb{T}, \tag{17a}$$

$$\sum_{\tau \in \mathbb{T}} \eta_k u_j^k(\tau) p_j^k(\tau) = \varepsilon_j^k, \quad \forall k \in \mathcal{K}, \forall j \in \mathcal{V}, \tag{17b}$$

$$p_j^k(\tau) \leq R_k^+, \quad \forall k \in \mathcal{K}, \forall k \in \mathcal{V}, \forall \tau \in \mathbb{T}, \tag{17c}$$

$$u_j^k(\tau) = \begin{cases} 1 & t_j^k \leq \tau \Delta_t \leq t_j^k + d_j^k - \Delta_t \\ & \text{and is charging} \\ 0 & \text{otherwise,} \end{cases} \quad \forall k \in \mathcal{K}, \forall j \in \mathcal{V}, \forall \tau \in \mathbb{T}. \tag{17d}$$

In (17d), $\tau\Delta_t \geq t_j^k$ means that the starting time of τ is no earlier than the arrival time of k at j. $\tau\Delta_t \leq t_j^k + d_j^k - \Delta_t$, or equivalently $\tau\Delta_t + \Delta_t \leq t_j^k + d_j^k$, means that time slot τ must end before the departure time of k at j.

In this implementation, $u_j^k(\tau)$ is conditioned on variables t_j^k and d_j^k, and cannot be properly modelled in the standard form. By using the same linearization technique employed to handle (7) and (11a) previously, we can re-write (17d) into:

$$u_j^k(\tau) \leq 1 - (t_j^k - \tau\Delta_t)/M, \tag{18a}$$

$$u_j^k(\tau) \leq 1 + (t_j^k + d_j^k - \Delta_t - \tau\Delta_t)/M, \quad \forall k \in \mathcal{K},\ \forall j \in \mathcal{V},\ \forall \tau \in \mathbb{T}. \tag{18b}$$

When $t_j^k \leq \tau\Delta_t \leq t_j^k + d_j^k - \Delta_t$, the RHS of the inequalities in (18) are equal to or greater than one, rendering $u_j^k(\tau) \in \{0, 1\}$. So we can determine through optimization if k should charge at τ ($u_j^k(\tau) = 1$) or simply stop at j without charging ($u_j^k(\tau) = 0$). For other τ values, the RHS of inequalities in (18) are smaller than one (but greater than zero). These τ's correspond to the time slots in which k is not staying at j, thus $u_j^k(\tau) = 0$.

E. Joint Routing and Charging Optimization

With the above simplifications, the AVLS joint routing and charging optimization can be formulated as follows:

Problem 1 (Joint Routing and Charging Problem):

$$\begin{aligned} &\text{minimize } D,\ -P, \text{ or } T \\ &\text{subject to } (4)\text{–}(6),\ (8)\text{–}(10),\ (11b),\ (15),\ (16), \\ &\qquad (17a)\text{–}(17c), \text{ and } (18) \end{aligned}$$

V. Distributed Route Optimization

Problem 1 is a quadratic-constrained mixed-integer linear programming (QCILP). As mentioned in Section I, the AV population is expected to grow very fast in the near future and this will enlarge the problem size. Moreover, to be demonstrated in Section VI, the computational time will increase drastically with the problem size if it is solved in a centralized manner. So a scalable solution method is more practical. To speed up the computational process, in this section we develop a distributed solution method via dual decomposition [41], [42].

A. Partial Lagrangian Relaxation

It is evident that all constraints of Problem 1 are separable with respect to AVs $\mathcal{K}$ except (17a). We first relax this constraint by introducing Lagrangian multipliers $\lambda_g^\tau \geq 0$ and construct the following partial Lagrangian for the three objective functions:

$$\begin{aligned} L_D &= D + \sum_{g\in\mathcal{G}}\sum_{\tau\in\mathbb{T}} \lambda_g^\tau \Big(\sum_{k\in\mathcal{K}} p_{v_g}^k(\tau) - \overline{\omega}_g(\tau)\Big) \\ &= \sum_{k\in\mathcal{K}} \Big(\sum_{(i,j)\in\mathcal{E}} D_{ij} x_{ij}^k + \sum_{g\in\mathcal{G}} \Theta_g\Big) - \Omega \end{aligned} \tag{19a}$$

$$\begin{aligned} L_P &= -P + \sum_{g\in\mathcal{G}}\sum_{\tau\in\mathbb{T}} \lambda_g^\tau \Big(\sum_{k\in\mathcal{K}} p_{v_g}^k(\tau) - \overline{\omega}_g(\tau)\Big) \\ &= -\sum_{k\in\mathcal{K}}\sum_{g\in\mathcal{G}} \big(\varepsilon_{v_g}^k - \Theta_g\big) - \Omega \end{aligned} \tag{19b}$$

$$\begin{aligned} L_T &= T + \sum_{g\in\mathcal{G}}\sum_{\tau\in\mathbb{T}} \lambda_g^\tau \Big(\sum_{k\in\mathcal{K}} p_{v_g}^k(\tau) - \overline{\omega}_g(\tau)\Big) \\ &= \sum_{k\in\mathcal{K}} \Big(t_{\overline{P}_k}^k + \sum_{g\in\mathcal{G}} \Theta_g\Big) - \Omega \end{aligned} \tag{19c}$$

where $\Theta_g = \sum_{\tau\in\mathbb{T}} \lambda_g^\tau p_{v_g}^k(\tau)$ and $\Omega = \sum_{g\in\mathcal{G}}\sum_{\tau\in\mathbb{T}} \lambda_g^\tau \omega_g(\tau)$. L_D, L_P, and L_T represent the partial Lagrangian of objective functions (1), (2), and (3), respectively. Given $\Lambda = \{\lambda_g^\tau | g \in \mathcal{G}, \tau \in \mathbb{T}\}$, the relaxed problem (named the primal problem in the sequel, whose optimal objective value is denoted by Z_P) can be constructed as follows:

Problem 2 (Relaxed Problem):

$$\begin{aligned} &\text{minimize } L_D,\ L_P, \text{ or } L_T \\ &\text{subject to } \delta \in \mathcal{X}' \end{aligned}$$

where $\mathcal{X}'$ is the solution space confined by all constraints of Problem 1 except (17a). Let $Z(\Lambda)$ be the optimal objective value and trivially $Z(\Lambda) \leq Z_P, \forall \Lambda \succeq 0$ provides a lower bound for the primal problem [42].

B. Dual Decomposition

In the relaxed problem, L_D, L_P, or L_T is not separable with respect to $\mathcal{K}$. To overcome this, we construct the corresponding dual functions as follows:

$$g(\Lambda) = \sum_{k\in\mathcal{K}} \inf_{\delta\in\mathcal{X}'} \{G_k(\delta, \Lambda)\} - \Omega, \tag{20}$$

where

$$G_k(\delta, \Lambda) = \begin{cases} \displaystyle\sum_{(i,j)\in\mathcal{E}} D_{ij} x_{ij}^k + \sum_{g\in\mathcal{G}} \Theta_g & \text{corresponds to } L_D \\ \displaystyle -\sum_{g\in\mathcal{G}} \big(\varepsilon_{v_g}^k - \Theta_g\big) & \text{corresponds to } L_P \\ \displaystyle t_{\overline{P}_k}^k + \sum_{g\in\mathcal{G}} \Theta_g(\tau) & \text{corresponds to } L_T. \end{cases}$$

Now $g(\Lambda)$ is a convex function because of the point-wise infimum of affine functions of Λ [41]. Given a fixed Λ, we can decompose the problem into a number of subproblems, each of which is given as follows:

Problem 3 (Sub-problem for k):

$$\begin{aligned} &\text{minimize } G_k(\delta, \Lambda) \\ &\text{subject to } \sum_{i\in\mathcal{V}} x_{ij}^k \geq 1, \quad \forall j \in \{P_q' | q \in \mathcal{Q}_k\}, \\ &\qquad \textstyle\sum_{i\in\mathcal{V}} x_{ij}^k - \sum_{i\in\mathcal{V}} x_{ji}^k = 0, \quad \forall j \in \mathcal{V} \setminus \{\underline{P}_k, \overline{P}_k\}, \\ &\qquad \textstyle\sum_{i\in\mathcal{V}} x_{ij}^k - \sum_{i\in\mathcal{V}} x_{ji}^k = 0, \quad \forall j \in \mathcal{V}, \underline{P}_k = \overline{P}_k, \\ &\qquad \textstyle\sum_{i\in\mathcal{V}} x_{ij}^k - \sum_{i\in\mathcal{V}} x_{ji}^k = -1, \quad j = \underline{P}_k, \underline{P}_k \neq \overline{P}_k, \\ &\qquad \textstyle\sum_{i\in\mathcal{V}} x_{ij}^k - \sum_{i\in\mathcal{V}} x_{ji}^k = 1, \quad j = \overline{P}_k, \underline{P}_k \neq \overline{P}_k, \\ &\qquad d_j^k \geq D_q', \quad \forall j \in \{P_q' | q \in \mathcal{Q}_k\}, \\ &\qquad \underline{T}_q' \leq t_j^k \leq \overline{T}_q', \quad \forall q \in \mathcal{Q}_k, j = P_q', \end{aligned}$$

$$
\begin{aligned}
&t^k_{\underline{P}_k} \le \overline{T}_k,\\
&\varepsilon^k_j \le d^k_j R^+_k, \quad \forall j \in \{v_g | g \in \mathcal{G}\} \cup \{v_d | d \in \mathcal{D}\},\\
&\varepsilon^k_j = 0, \quad \forall j \notin \{v_g | g \in \mathcal{G}\} \cup \{v_d | d \in \mathcal{D}\},\\
&t^k_j \ge t^k_i + d^k_i + L_{ij} - M(1 - x^k_{ij}),\\
&\qquad \forall i \in \mathcal{V},\ \forall j \in \mathcal{V} \setminus \underline{P}_k,\\
&c^k_j \le c^k_i + (\varepsilon^k_i - D_{ij} R^{ij-}_k)/B_k + M(1 - x^k_{ij}),\\
&\qquad \forall i \in \mathcal{V},\ \forall j \in \mathcal{V} \setminus \underline{P}_k,\\
&c^k_j \ge c^k_i + (\varepsilon^k_i - D_{ij} R^{ij-}_k)/B_k - M(1 - x^k_{ij}),\\
&\qquad \forall i \in \mathcal{V}, \forall j \in \mathcal{V} \setminus \underline{P}_k,\\
&\sum\nolimits_{\tau \in \mathbb{T}} \eta_k u^k_j(\tau) p^k_j(\tau) = \varepsilon^k_j, \quad \forall j \in \mathcal{V},\\
&p^k_j(\tau) \le R^+_k, \quad \forall j \in \mathcal{V},\ \forall \tau \in \mathbb{T},\\
&u^k_j(\tau) \le 1 - (t^k_j - \tau \Delta_t)/M, \quad \forall j \in \mathcal{V},\ \forall \tau \in \mathbb{T},\\
&u^k_j(\tau) \le 1 + (t^k_j + d^k_j - \Delta_t - \tau \Delta_t)/M,\\
&\qquad \forall j \in \mathcal{V},\ \forall \tau \in \mathbb{T}.
\end{aligned}
$$

Then we construct the dual problem to update Λ as:

Problem 4 (Dual Problem):

$$
\begin{aligned}
\text{maximize} \quad & \sum_{k \in \mathcal{K}} G^*_k(\delta, \Lambda) - \Omega\\
\text{subject to} \quad & \Lambda \succeq 0,
\end{aligned}
$$

where $G^*_k(\delta, \Lambda)$ is the optimal value to Problem 3. The optimal solutions for Problem 4 can be employed to recover the solution to the primal Problem 1, which will be introduced next.

C. Projected Gradient Descent and Implementation

Problem 4 is linear. When given $G^*_k(\delta, \Lambda)$ by solving Problem 3, Problem 4 can be effectively solved with the Projected Gradient Descent (PGD) method [42], which is an iterative method to effectively solve the dual problem. In each iteration, PGD maximizes the objective function by moving a candidate solution in the gradient direction of the function:

$$
\frac{\partial g(\Lambda)}{\partial \lambda^\tau_g} = \frac{\partial \left(\sum_{k \in \mathcal{K}} \sum_{g \in \mathcal{G}} \Theta_g - \Omega\right)}{\partial \lambda^\tau_g} = \sum_{k \in \mathcal{K}} p^k_{v_g}(\tau) - \overline{\omega}_g(\tau). \tag{21}
$$

The optimal values for Λ can be approached by the following update rule:

$$
\lambda^\tau_g(i+1) = \left[\lambda^\tau_g(i) + \alpha^\tau_g(i) \times \Big(\sum_{k \in \mathcal{K}} p^{k*}_{v_g}(\tau, i) - \overline{\omega}_g(\tau)\Big)\right]^+, \tag{22}
$$

where $\lambda^\tau_g(i)$ stands for the value of λ^τ_g at the i-th iteration, $\alpha^\tau_g(i) > 0$ is the step size, and $p^{k*}_{v_g}(\tau, i)$ is the optimal value of $p^k_{v_g}(\tau)$ in Problem 3 at the i-th iteration. If we have $\sum_{k \in \mathcal{K}} p^{k*}_{v_g}(\tau, i) > \overline{\omega}_g(\tau)$ which violates (17a), (22) will make $\lambda^\tau_g(i+1)$ greater than $\lambda^\tau_g(i)$, leading to smaller $p^{k*}_{v_g}(\tau, i+1)$ values in the next iteration.

By PGD, the most computationally expensive part of the problem can be distributed to the vehicles. Fig. 2 depicts the structure of the distributed algorithm and how the components

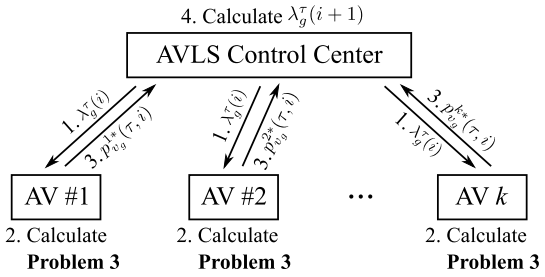

Fig. 2. Implementation of distributed projected gradient descent solution.

cooperate to solve the dual problem in an iterative manner. At the beginning of the i-th iteration, the control center broadcasts $\lambda^\tau_g(i)$ to all vehicles in the system (Step 1 in Fig. 2). Upon receiving the information, each vehicle solves Problem 3 independently using their local information (Step 2), and the optimal $p^{k*}_{v_g}(\tau, i)$ values are then reported back to the control center (Step 3). Eventually, when all $p^{k*}_{v_g}(\tau, i)$ values have been received, the control center updates $\lambda^\tau_g(i+1)$ using (22) (Step 4). We consider PGD converged if

$$
\sum_{k \in \mathcal{K}} \frac{\left| \sum_{g \in \mathcal{G}} \sum_{\tau \le \tau^{\max}} p^{k*}_{v_g}(\tau, i+1) - \sum_{g \in \mathcal{G}} \sum_{\tau \le \tau^{\max}} p^{k*}_{v_g}(\tau, i) \right|}{\sum_{g \in \mathcal{G}} \sum_{\tau \le \tau^{\max}} p^{k*}_{v_g}(\tau, i+1)} < \epsilon, \tag{23}
$$

where ϵ is the termination threshold, which has a small positive value, e.g., 10^{-4}.

The primal solution of the original Problem 1 can be recovered from the solutions to the sub-problems collectively. Simply combining all sub-problem solutions may produce a solution 1 violating (17a). If so, we first identify all combinations of $g \in \mathcal{G}$ and $\tau \in \mathbb{T}$ that violate the constraint. For each pair of (g, τ), all vehicles charged at g at time slot τ are sorted by their charging powers, i.e., $p^{k*}_{v_g}(\tau)$. Then we reduce these charging powers one by one until the constraint is satisfied. For instance, suppose $p^{\mathrm{A}*}_{v_g}(\tau)$, $p^{\mathrm{B}*}_{v_g}(\tau)$, $p^{\mathrm{C}*}_{v_g}(\tau)$, $\cdots$ are the charging powers at g at time slot τ, sorted in a descending order. The charging power of vehicle A is first replaced by that of B. In other words, we reduce the largest charging power to the second largest. If (17a) is still violated, the second largest charging power is reduced to the third largest. This process repeats until (17a) is satisfied, i.e., $\sum_{k \in \mathcal{K}} p^k_{v_g}(\tau) \le \overline{\omega}_g(\tau)$. In cases that all charging powers are reduced but the constraint is still not violated, we restart this process. In the worst case, all charging power values will be reduced to zero, and (17a) must be eventually satisfied. A feasible primal solution can then be constructed as the final solution to Problem 1.

This distributed method incurs minimal information exchange between the vehicles and the control center. In each iteration, instead of reporting all decision variables back to the control center, each vehicle only needs to send its $p^{k*}_{v_g}(\tau, i)$. For a practical system with a large fleet of AVs, this method can effectively prevent a large amount of redundant information, such as traffic information and vehicular data, from being gathered at the control center. In addition, distributing the sub-problems to the vehicles can significantly

speed up the computation process, which will be illustrated in Section VI.

VI. Case Studies

We conduct three tests to evaluate the performance of our proposed system. We first assess the performance of AVLS routing and charging optimization on different network sizes using synthetic transportation networks. Then we test the system performance on different vehicle fleet sizes and numbers of logistic requests with a real-world transportation system. Next we further examine the convergence behavior of the distributed solution method. Finally, we investigate the impact of time slot duration Δ_t on the solution optimality and computational time.

A. Simulation Configurations

Consider that each vehicle can be charged at any of DGs in the system with charging rate capped by 22kW [43]. The vehicles are equipped with batteries having random charging efficiency from 80% to 90% and the battery capacities are randomly selected from 24kWh, 30kWh (Nissan Leaf [44]), 40kWh, 60kWh, 70kWh, 85kWh, and 90kWh (Tesla Model S [45]). According to the analysis in [46], the most dominating factor that influences electric motor energy consumption is the travel distance, followed by vehicular parameters (mass, rolling resistance, etc.) and road parameters (gradient angle, road friction, etc.). Hence, the energy consumption for each vehicle on (i, j) is set to a random value between $0.3D_{ij}$ to $1.0D_{ij}$, which loosely resembles the trend given in [46, eq. (1)]. The service time for each request is set between 5 and 30 minutes, which are typical values in the benchmark test cases available at [47].

In all test cases, it is assumed that $\lceil |\mathcal{V}|/3 \rceil$ DGs are randomly located in the networks. We adopt the Eastern and Western Wind Integration Data Set [48] provided by National Renewable Energy Laboratory to simulate the energy generation of DGs, in which the wind power generations around Los Angeles are employed. As the provided power outputs are too large (0.1-10 MW) for typical-size DGs, the profiles are scaled down such that the maximum power output is less than 50kW [49].

In addition, $|\mathcal{V}|/25$ depots are also randomly located in the networks. Each AV is initially located at a random depot with SOC randomly set between 30% and 70%. Their final destinations are randomly selected, different from their starting positions. Each AV serves a random amount of requests, whose destinations are randomly selected among the nodes. The deadlines of these requests are set to a random value between one and three hours and the deadline for the AV to reach its final destination equals to the latest deadline of all its logistic requests. We do not prioritize the requests with specific factors except their delivery deadlines. In our design, the order of service for all requests by the same AV is solely generated according to the result of the optimization, which depends on the request deadlines and the underlying transportation system traffic conditions. It is possible that some requests do have higher/more urgent priority in a real-world system. For such cases, tighter delivery deadlines can be assigned to these requests in the model to realize the emergent cases. The length of time slot Δ_t is set to one minute.

We perform the simulations on a computer with an Intel Core i7 CPU at 3.60 GHz and 32 GB RAM. The testing code is developed in Python 3 and the optimization problems are solved using Gurobi optimization solver [40].

By following [16], the step size of the distributed method is updated as follows: $\alpha_g^\tau(0)$ is initialized with zero value. $\alpha_g^\tau(i+1) = \alpha_g^\tau(i) \times 1.1$ if $\sum_{k\in\mathcal{K}} \rho_{vg}^{k*}(\tau, i) < \sum_{k\in\mathcal{K}} \rho_{vg}^{k*}(\tau, i-1)$, and $\alpha_g^\tau(i+1) = \alpha_g^\tau(i) \times 0.1$ otherwise. In addition, a step size cap $\overline{\alpha}_g^\tau(i) = 0.1 \times (1 - 10^{-3})^i$ is introduced for $\alpha_g^\tau(i)$. This satisfies the "non-summable diminishing step size rule", which guarantees convergence of the distributed algorithm [41]. The one-way communication delay is assumed to be 100 ms, which is set according to the average latency of practical cellular systems [16], [50].

B. Impact of Network Size

We investigate the impact of transportation network size to the route scheduling performance. Random cases with different numbers of road intersections ($|\mathcal{V}|$) are generated and we compare two methods to solve the joint routing and charging problem: (i) solving Problem 1 in the centralized manner and (ii) the distributed solution method discussed in Section V. The results in terms of objective function value and computational time for both methods are illustrated for comparison.

For all the random cases, each node in the road network connects to its nearest two to four nodes by two-way roads. We consider 50 AVs, each of which serves three to five logistic requests to simulate different load capacity of vehicles. The driving speed of each vehicle is dynamic and it varies according to the traffic speed of the traversing road. In other words, the driving speed is set to the traffic flow rate of each particular road. The traffic speed of each road is assigned according to the real-world data of downtown Cologne, Germany during 7am to 8am[3] [51], [52]. 5km × 5km, respectively.

The simulation results are summarized in Fig. 3. As the centralized method provides the best achievable solution, we show the optimality of the distributed method in relative percentage with respect to the centralized approach. For both objectives of minimizing travel distance and delivery time, their optimalities are calculated by $F^{\text{ctr}}/F^{\text{dst}} \times 100\%$, where F^{ctr} and F^{dst} are the optimal objective function values for the centralized and distributed solutions, respectively. For maximizing charged DG energy, the optimality is calculated by $F^{\text{dst}}/F^{\text{ctr}}$. We also provide the actual values for the centralized method (in brackets) in the figure for reference.

From Fig. 3 it can be observed that, for both the travel distance and delivery time, there is no significant relationship between the optimal value and the network size. The main reason is that in a fixed area, the average driving distance between two locations is generally unaffected even with more nodes defined in the graph, so as the driving time. On the other hand, the total charged DG energy increases

[3]7–8 am is selected because this period is among the time periods with the most vehicular traces in the dataset, leading to a more realistic traffic scenario.

TABLE II
MINIMIZED TRAVEL DISTANCE WITH DIFFERENT NUMBER OF AVS AND LOGISTIC REQUESTS

Number of vehicles	20	50	100	200	300	50			
Number of requests	3∼5					1∼2	2∼3	3∼5	4∼7
Centralized result	12.24	32.07	67.11	133.11	202.24	12.56	18.98	32.07	45.10
Distributed optimality	99.39%	99.51%	99.55%	99.66%	99.64%	99.22%	99.40%	99.51%	99.31%
Centralized time (s)	112.39	279.92	891.76	2856.00	6516.49	95.01	176.88	279.92	355.06
Distributed time (s)	51.53	61.12	106.56	229.87	405.56	17.22	38.82	61.12	111.70
Distributed speedup ratio	2.18	4.58	8.37	12.42	16.07	5.52	4.56	4.58	3.18

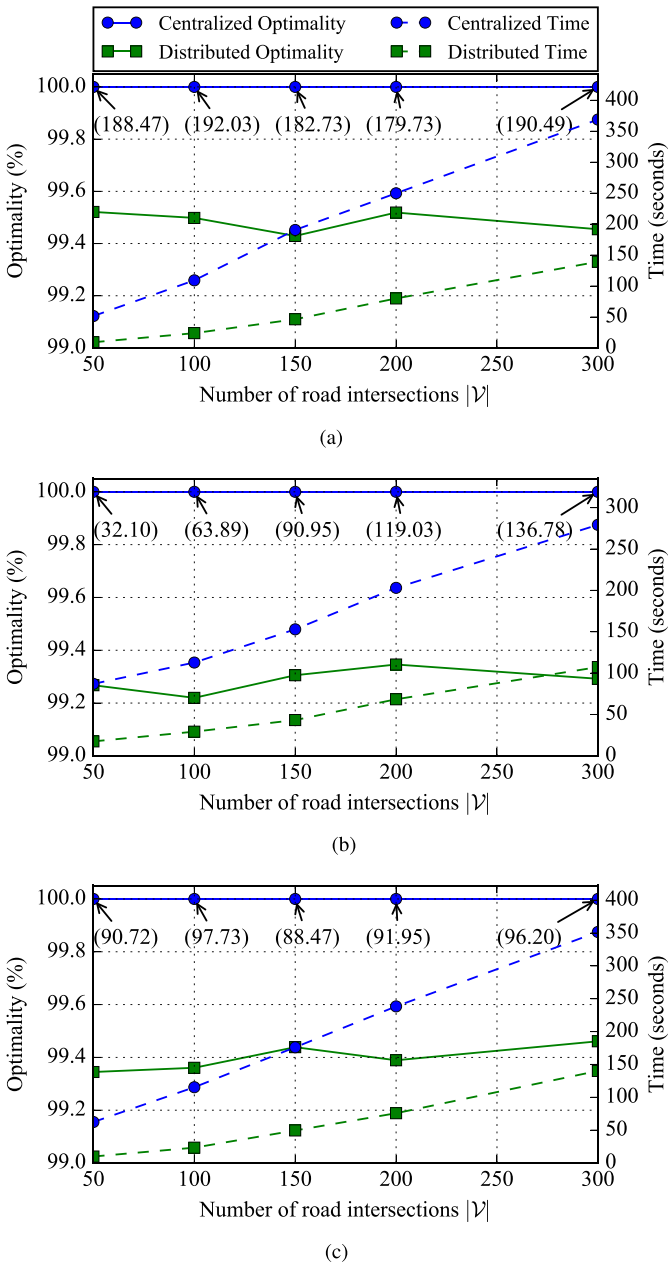

Fig. 3. Objective function value optimality and computation times with different numbers of road intersections. (a) Minimizing travel distance (1). (b) Maximizing DG energy (2). (c) Minimizing delivery time (3).

almost linearly with the network size. This is because that the number of DGs is proportional to the total number of nodes. More nodes lead to more DGs, which provide more energy for charging. The optimality of the distributed solution are outstanding with less than 0.8% optimality gaps. The optimality is fluctuating due to the randomness in generating different network topologies but the degree of fluctuation is actually insignificant. At the same time, the simulation time for both methods increases with $|\mathcal{V}|$. This is contributed by the increasing complexity of transportation network, which introduces more constraints to the optimization problem.

C. Impact of Fleet Size and Number of Logistic Requests

Besides the network size, the number of AVs and logistic requests can also significantly influence the system performance. In this test, we study how they impact on a real-world transportation system. We adopt the map data of downtown Cologne, Germany from OpenStreepMap [53] to construct a road network of the area. Specifically, all primary, secondary, tertiary, and residential roads/paths are extracted to construct a graph as depicted in Fig. 4. Over the graph, we employ the vehicular mobility trace of 7am to 8 am from [51] and [52] to determine the average traffic speed of each road in the network. The subsequent simulations simulations are conduced on this real-world setting. For conciseness, we present the simulation results for the objective of minimizing travel distance only. The results of the other objectives are given in Appendix B.

We first study the influence of AV fleet size to the system performance. Here we generate 50 random problem cases for each of $|\mathcal{K}| \in \{20, 50, 100, 200, 300\}$. All other configurations are identical to the description in Section VI-A. The averaged simulation results are presented in Table II. It can be observed that the optimal objective function values increase roughly linearly with the fleet size. This is because the average individual travel distance of each AV are not influenced by the increasing size of the fleet. Hence with more AVs, the total travel distance also proportionally increase. In addition, the optimality of the distributed solution improves with the number of AVs. The reason is that more AVs provide larger flexibility, and the distributed algorithm can generate better solution much easier.

By the centralized approach, the computational time increases drastically with $|\mathcal{K}|$. But that for the distributed solution is relatively insignificant. The reason is that, although more vehicles result in more sub-problems, they can be solved in a parallel manner. For each sub-problem, the problem size is unrelated to the fleet size, leading to steady computational time. However, as illustrated in Section VI-D, the number of iterations required for the distributed solution to converge actually increases with fleet size. The reason is that it takes more time to coordinate more sub-problems for convergence.

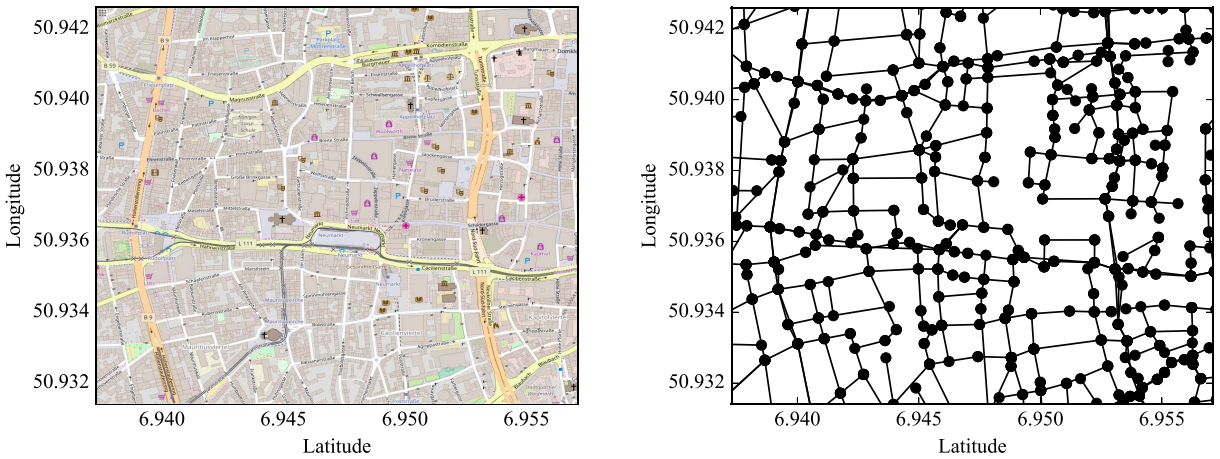

Fig. 4. The downtown map and road network of Cologne. (a) Cologne downtown map. (b) Cologne downtown road network.

Therefore, an increase in total computation time can still be observed. Despite this, the results still demonstrate the efficiency of the proposed distributed solution in developing routing and charging plans for the AVs in the system. In real-world implementations, when it comes to true optimal solution, we should go for the centralized solution but its computational time increases exponentially with the AV fleet size. With stringent computational time requirements, the distributed solution is preferable for producing high-quality results.

Next, we examine the sensitivity of the number of logistic requests each AV serves. We consider four scenarios in which the number of logistic requests for each vehicle is randomly generated from one to two, from two to three, from three to five, or from four to seven. For each scenario, 50 random cases are generated, and the results are presented in Table II.

In general, the optimal objective value follows a similar trend as that on changing the fleet size. The computational time required grows linearly with the number of requests. Meanwhile, the optimality of the distributed solution is not significantly influenced by the number of requests. This is due to the fact that increasing logistic requests does not change the number of sub-problems created, which does not change the solution space of Λ in Problem 4.

D. Convergence of Distributed Solution

In this test, we study the convergence of the distributed algorithm. We select two arbitrary test cases of 20 and 300 vehicles from Section VI-C for illustration. We consider maximizing the total charged DG and the corresponding primal and dual objective values computed by PGD in each iterations are plotted in Fig. 5. It shows that the distributed algorithm converges very fast (in 11th and 21st iterations for the 20- and 300-vehicle cases, respectively). In both cases, the duality gap diminishes when the algorithm terminates. In addition, the convergence speed in the larger test case is relatively slower. In fact, increasing the number of AVs will also enlarge the solution space of Λ rendering it more difficult to solve. After being convergent, the duality gap for the larger case is also relatively smaller. This is consistent with the previous result given in Table II.

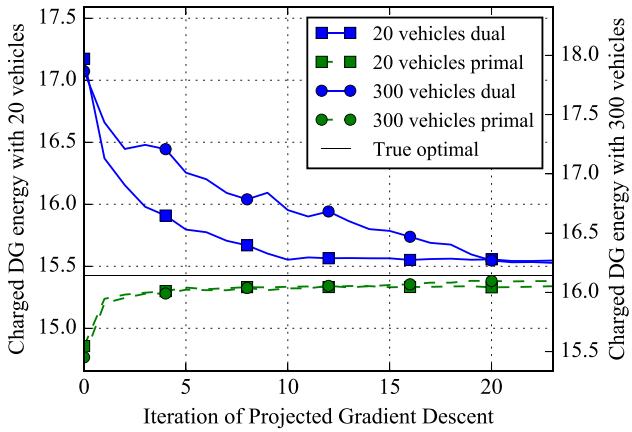

Fig. 5. Primal and dual convergence of the distributed solution on solving test cases with 20 and 300 vehicles.

TABLE III
PERFORMANCE COMPARISON WITH VARIOUS TIME SLOT LENGTHS

Δ_t	15 s	30 s	1 min	2 min
Optimality	100%	>99.99%	>99.99%	99.99%
Time (s)	544.58	196.17	112.39	105.25
Δ_t	5 min	10 min	30 min	1 hr
Optimality	99.88%	97.70%	93.91%	85.73%
Time (s)	101.60	100.13	99.44	99.37

E. Time Slot Duration

In this test we investigate the impact of time slot duration Δ_t on the optimality and computational time. Recall that in Section IV-D, we divide time into slots of length Δ_t to approximate the continuous time horizon in Constraints (12)–(14). Finer granularity makes better approximation, but it results in higher complexity.

We adopt the 50 test cases with 20 vehicles generated in Section VI-C in this test. For each case, we consider Δ_t to

TABLE IV
MAXIMIZED DG ENERGY WITH DIFFERENT NUMBER OF AVS AND LOGISTIC REQUESTS

Number of vehicles	20	50	100	200	300	50			
Number of requests	3∼5					1∼2	2∼3	3∼5	4∼7
Centralized result	15.17	15.28	15.52	15.04	15.49	15.22	15.29	15.28	15.04
Distributed optimality	99.11%	99.30%	99.54%	99.64%	99.77%	99.11%	99.30%	99.30%	99.30%
Centralized time (s)	143.97	330.89	1225.87	3290.71	6732.22	143.38	225.59	330.89	450.91
Distributed time (s)	72.86	84.71	171.71	280.22	419.97	28.90	58.41	84.71	151.82
Distributed speedup ratio	1.98	3.90	7.14	11.74	16.03	4.96	3.86	3.90	2.97

TABLE V
MINIMIZED DELIVERY TIME WITH DIFFERENT NUMBER OF AVS AND LOGISTIC REQUESTS

Number of vehicles	20	50	100	200	300	50			
Number of requests	3∼5					1∼2	2∼3	3∼5	4∼7
Centralized result	19.38	45.91	92.82	199.65	300.00	26.58	39.95	45.91	60.02
Distributed optimality	99.28%	99.36%	99.50%	99.65%	99.81%	99.29%	99.35%	99.36%	99.40%
Centralized time (s)	85.97	265.39	758.20	2442.88	5140.29	100.60	158.27	265.39	316.67
Distributed time (s)	34.66	53.67	105.65	194.62	343.26	15.94	31.24	53.67	102.51
Distributed speedup ratio	2.48	4.94	7.17	12.55	14.97	6.31	5.06	4.94	3.08

be 15 seconds, 30 seconds, 1 minute, 2 minutes, 5 minutes, 10 minutes, 30 minutes, and 1 hour. For demonstration, we focus on maximizing charged DG energy and the centralized solution is employed to produce the optimal results. As $\Delta_t = 15$s has the best performance, all results are presented in percentage relative to $\Delta_t = 15$ s shown in Table III.

From the results it can be concluded that the optimality drops with Δ_t. When Δ_t is smaller ($\leq$1 min), the relative optimality can reach greater than 99.99%. The performance deteriorates significantly with coarser time slots (say $\Delta_t >$ 10min). When an AV is assigned to get charged in a time slot, it needs to stay at that DG for the complete time slot. When Δ_t is too large, a long stay may prevent the vehicle from delivering goods on time. The optimization may prevent charging at critical time slots rendering a smaller total charged DG energy. Table III also gives the corresponding computational time required to develop the optimal solutions. While coarse divisions do not significantly reduce the time, fine-grained time resolutions lead to drastically increase of computational time. Therefore, there is a trade-off between solution quality and computational time.

VII. CONCLUSION

With introduction of AVs to modern transportation systems, they can be used to accommodate logistic requests effectively in future smart cities. As most AVs are powered by electricity, they can help improve renewable penetrations by coordinating their charging needs. In this paper, we develop AVLS to integrate the logistics system with AVs in consideration of their charging capabilities. In AVLS, AVs traverse a city to serve logistic requests. Along their routes, AVs can stay at one or multiple DGs to get charged. This can not only substantially lengthen their driving distance but also allows the AVs to participate in V2G. We focus on how to optimally develop the routing and charging plans of the governed AVs. We formulate the corresponding quadratic-constrained optimization problem but it suffers from scalability issues. To make it more practical, we develop a distributed solution method via dual decomposition. We conduct extensive simulations to assess the performance of the proposed AVLS. We investigate the impact of problem size on the system performance and the required computational time. The simulation results evidently show that the distributed solution can produce nearly optimal solutions with drastic reduction on computational time. In addition, we analyze the convergence of the distributed method and the results show that the convergence speed is closely related to the number of vehicles in the system.

For future work, we will extend the deterministic formulation with a stochastic model. We will also investigate how to integrate the intelligent transportation system with smart grid seamlessly for a sustainable smart city.

APPENDIX A
FORMULATING FORBIDDEN ROADS AND NODES

In real-world implementation, it is possible that some vehicles cannot pass through certain roads or visit certain locations. In other words, particular (types of) vehicles may be forbidden to reach a subset of edges/nodes in the transportation system. We can model this by incorporating additional constraints to Problem 1. Suppose AV k is forbidden from running over road (i, j). Recall that x_{ij}^k defines if k drives on (i, j) along its route. We can model its forbiddance on (i, j) by $x_{ij}^k = 0$. For k's forbiddance on a particular node i, we can simply set x_{ij}^k of all the connecting roads to zeros. An alternative and more computationally efficient way is to set k's visiting time at i to zero, i.e., $t_i^k = 0$. This means that k cannot visit i (c.f. (7)). Finally, in case that k is only allowed to visit j in a specified period of time, for instance, from $\underline{T}$ to $\overline{T}$, we can include the limit $\underline{T} \leq t_j^k \leq \overline{T}$.

APPENDIX B
IMPACT OF FLEET SIZE AND NUMBER OF LOGISTIC REQUESTS ON DG ENERGY UTILIZATION AND DELIVERY TIME

Related to Section VI-C, the simulation results with respect to the optimal values of DG energy utilization and delivery

time are presented. The simulation configurations are identical to those adopted in Section VI-C and the results are summarized in Tables IV and V. The maximized DG energy utilization is generally insensitive to either fleet size or number of logistic requests. This is because the total excessive energy available at DGs is constant. Thus increasing the number of AVs cannot further increase the amount of energy charged from the DGs. Similarly, the minimized delivery time follows the same trend as the result presented in Table II. The analysis in Section VI-C is also applicable to this objective.

REFERENCES

[1] H. Hackmann, S. C. Moser, and A. L. S. Clair, "The social heart of global environmental change," *Nature Clim. Change*, vol. 4, no. 8, pp. 653–655, Jul. 2014.

[2] A. Zanella, N. Bui, A. Castellani, L. Vangelista, and M. Zorzi, "Internet of Things for smart cities," *IEEE Internet Things J.*, vol. 1, no. 1, pp. 22–32, Feb. 2014.

[3] D. Mohr, H.-W. Kaas, P. Gao, D. Wee, and T. Möller, "Automotive revolution—Perspective towards 2030: How the convergence of disruptive technology-driven trends could transform the auto industry," McKinsey & Company, Washington, DC, USA, Tech. Rep., Jan. 2016.

[4] T. Litman, "Autonomous vehicle implementation predictions: Implications for transport planning," Victoria Transp. Policy Inst., Victoria, BC, Canada, Tech. Rep. 15-3326, Feb. 2017.

[5] Z. Qu, *Control of Dynamical Systems: Applications to Autonomous Vehicles*. New York, NY, USA: Springer, 2009.

[6] P.-O. Groß, M. Geisinger, J. F. Ehmke, and D. C. Mattfeld, "Interval travel times for more reliable routing in city logistics," *Transp. Res. Proc.*, vol. 12, pp. 239–251, Jan. 2016.

[7] T. G. Crainic, "City logistics," in *State-of-the-Art Decision-Making Tools in the Information-Intensive Age* (INFORMS Tutorials in Operations Research). Catonsville, MD, USA: INFORMS, Sep. 2008, pp. 181–212.

[8] A. Papavasiliou, S. S. Oren, and R. P. O'Neill, "Reserve requirements for wind power integration: A scenario-based stochastic programming framework," *IEEE Trans. Power Syst.*, vol. 26, no. 4, pp. 2197–2206, Nov. 2011.

[9] H. Yang *et al.*, "Operational planning of electric vehicles for balancing wind power and load fluctuations in a microgrid," *IEEE Trans. Sustain. Energy*, vol. 8, no. 2, pp. 592–604, Apr. 2017.

[10] A. Y. Saber and G. K. Venayagamoorthy, "Plug-in vehicles and renewable energy sources for cost and emission reductions," *IEEE Trans. Ind. Electron.*, vol. 58, no. 4, pp. 1229–1238, Apr. 2011.

[11] J. M. Guerrero, M. Chandorkar, T.-L. Lee, and P. C. Loh, "Advanced control architectures for intelligent microgrids—Part II: Power quality, energy storage, and AC/DC microgrids," *IEEE Trans. Ind. Electron.*, vol. 60, no. 4, pp. 1263–1270, Apr. 2013.

[12] R. Arnay *et al.*, "Safe and reliable path planning for the autonomous vehicle Verdino," *IEEE Intell. Transp. Syst. Mag.*, vol. 8, no. 2, pp. 22–32, Apr. 2016.

[13] B. Li, H. Du, and W. Li, "A potential field approach-based trajectory control for autonomous electric vehicles with in-wheel motors," *IEEE Trans. Intell. Transp. Syst.*, vol. 18, no. 8, pp. 2044–2055, Aug. 2017.

[14] R. Hult, G. R. Campos, E. Steinmetz, L. Hammarstrand, P. Falcone, and H. Wymeersch, "Coordination of cooperative autonomous vehicles: Toward safer and more efficient road transportation," *IEEE Signal Process. Mag.*, vol. 33, no. 6, pp. 74–84, Nov. 2016.

[15] J. Nie, J. Zhang, W. Ding, X. Wan, X. Chen, and B. Ran, "Decentralized cooperative lane-changing decision-making for connected autonomous vehicles," *IEEE Access*, vol. 4, pp. 9413–9420, 2016.

[16] A. Lam, J. J. Q. Yu, Y. Hou, and V. O. K. Li, "Coordinated autonomous vehicle parking for vehicle-to-grid services: Formulation and distributed algorithm," *IEEE Trans. Smart Grid*. [Online]. Available: http://ieeexplore.ieee.org/document/7822948/

[17] H. N. T. Nguyen, C. Zhang, and J. Zhang, "Dynamic demand control of electric vehicles to support power grid with high penetration level of renewable energy," *IEEE Trans. Transport. Electrific.*, vol. 2, no. 1, pp. 66–75, Mar. 2016.

[18] S. Shao, M. Pipattanasomporn, and S. Rahman, "Demand response as a load shaping tool in an intelligent grid with electric vehicles," *IEEE Trans. Smart Grid*, vol. 2, no. 4, pp. 624–631, Dec. 2011.

[19] Z. Fan, "A distributed demand response algorithm and its application to PHEV charging in smart grids," *IEEE Trans. Smart Grid*, vol. 3, no. 3, pp. 1280–1290, Sep. 2012.

[20] J. Donadee and M. D. Ilić, "Stochastic optimization of grid to vehicle frequency regulation capacity bids," *IEEE Trans. Smart Grid*, vol. 5, no. 2, pp. 1061–1069, Mar. 2014.

[21] J. A. P. Lopes, F. J. Soares, and P. M. R. Almeida, "Integration of electric vehicles in the electric power system," *Proc. IEEE*, vol. 99, no. 1, pp. 168–183, Jan. 2011.

[22] E. Sortomme and M. A. El-Sharkawi, "Optimal scheduling of vehicle-to-grid energy and ancillary services," *IEEE Trans. Smart Grid*, vol. 3, no. 1, pp. 351–359, Mar. 2012.

[23] W. Shuai, P. Maillé, and A. Pelov, "Charging electric vehicles in the smart city: A survey of economy-driven approaches," *IEEE Trans. Intell. Transp. Syst.*, vol. 17, no. 8, pp. 2089–2106, Aug. 2016.

[24] H. Quak, N. Nesterova, and T. van Rooijen, "Possibilities and barriers for using electric-powered vehicles in city logistics practice," *Transp. Res. Proc.*, vol. 12, pp. 157–169, Feb. 2016.

[25] Z. He, P. Chen, H. Liu, and Z. Guo, "Performance measurement system and strategies for developing low-carbon logistics: A case study in China," *J. Cleaner Prod.*, vol. 156, pp. 395–405, Jul. 2017.

[26] G. Duarte, C. Rolim, and P. Baptista, "How battery electric vehicles can contribute to sustainable urban logistics: A real-world application in Lisbon, Portugal," *Sustain. Energy Technol. Assessments*, vol. 15, pp. 71–78, Jun. 2016.

[27] A. Y. S. Lam, Y. W. Leung, and X. Chu, "Autonomous-vehicle public transportation system: Scheduling and admission control," *IEEE Trans. Intell. Transp. Syst.*, vol. 17, no. 5, pp. 1210–1226, May 2016.

[28] A. Y. S. Lam, "Combinatorial auction-based pricing for multi-tenant autonomous vehicle public transportation system," *IEEE Trans. Intell. Transp. Syst.*, vol. 17, no. 3, pp. 859–869, Mar. 2016.

[29] J. J. Q. Yu and A. Y. S. Lam, "Core-selecting auctions for autonomous vehicle public transportation system," submitted for publication.

[30] W. Shi, X. Xie, C. C. Chu, and R. Gadh, "Distributed optimal energy management in microgrids," *IEEE Trans. Smart Grid*, vol. 6, no. 3, pp. 1137–1146, May 2015.

[31] K. Rahbar, J. Xu, and R. Zhang, "Real-time energy storage management for renewable integration in microgrid: An off-line optimization approach," *IEEE Trans. Smart Grid*, vol. 6, no. 1, pp. 124–134, Jan. 2015.

[32] D. Simchi-Levi, P. Kaminsky, and E. Simchi-Levi, *Designing and Managing the Supply Chain*, 3rd ed. Boston, MA, USA: McGraw-Hill, Jul. 2007.

[33] A. Holzapfel, H. Kuhn, and M. G. Sternbeck, "Product allocation to different types of distribution center in retail logistics networks," *Eur. J. Oper. Res.*, vol 264, no. 3, pp. 948–966.

[34] R. A. Vasco and R. Morabito, "The dynamic vehicle allocation problem with application in trucking companies in Brazil," *Comput. Oper. Res.*, vol. 76, pp. 118–133, Dec. 2016.

[35] Y. Seyedi, H. Karimi, and S. Grijalva, "Distributed generation monitoring for hierarchical control applications in smart microgrids," *IEEE Trans. Power Syst.*, vol. 32, no. 3, pp. 2305–2314, May 2017.

[36] D. Jiang and L. Delgrossi, "IEEE 802.11p: Towards an international standard for wireless access in vehicular environments," in *Proc. IEEE Veh. Technol. Conf. (VTC Spring)*, May 2008, pp. 2036–2040.

[37] E. C. Eze, S. Zhang, and E. Liu, "Vehicular ad hoc networks (VANETs): Current state, challenges, potentials and way forward," in *Proc. 20th Int. Conf. Autom. Comput. (ICAC)*, Sep. 2014, pp. 176–181.

[38] A. Abdulaal, M. H. Cintuglu, S. Asfour, and O. A. Mohammed, "Solving the multivariant EV routing problem incorporating V2G and G2V options," *IEEE Trans. Transport. Electrific.*, vol. 3, no. 1, pp. 238–248, Mar. 2017.

[39] J. Lin, W. Zhou, and O. Wolfson, "Electric vehicle routing problem," *Transp. Res. Proc.*, vol. 12, pp. 508–521, Jan. 2016.

[40] *Gurobi Optimization*. Accessed: Apr. 16, 2017. [Online]. Available: http://www.gurobi.com/

[41] D. P. Bertsekas, *Nonlinear Programming*, 2nd ed. Belmont, MA, USA: Athena Scientific, Sep. 1999.

[42] S. Boyd and L. Vandenberghe, *Convex Optimization*, 1st ed. Cambridge, U.K.: Cambridge Univ. Press, Mar. 2004.

[43] *EV Solutions—Electric Vehicle Charging Products & Services*. Accessed: Apr. 16, 2017.[Online]. Available: http://www.evsolutions.com/

[44] *Nissan Leaf Review—Research New & Used Nissan Leaf Models*. Accessed: Apr. 16, 2017. [Online]. Available: https://www.edmunds.com/nissan/leaf/
[45] *Model S-Tesla Hong Kong*. Accessed: Apr. 16, 2017. [Online]. Available: https://www.tesla.com/en_HK/models
[46] C. De Cauwer, J. Van Mierlo, and T. Coosemans, "Energy consumption prediction for electric vehicles based on real-world data," *Energies*, vol. 8, no. 8, pp. 8573–8593, Aug. 2015.
[47] *Multiple Depot VRP Instances—Vehicle Routing Problem*. [Online]. Available: http://neo.lcc.uma.es/vrp/vrp-instances/multiple-depot-vrp-instances/
[48] *NREL—Eastern and Western Data Sets*. [Online]. Available: https://www.nrel.gov/grid/eastern-western-wind-data.html
[49] K. Strunz, E. Abbasi, and D. N. Huu, "DC microgrid for wind and solar power integration," *IEEE J. Emerg. Sel. Topics Power Electron.*, vol. 2, no. 1, pp. 115–126, Mar. 2014.
[50] (Feb. 2014). *3G/4G Wireless Network Latency: Comparing Verizon, AT&T, Sprint and T-Mobile*. [Online]. Available: http://www.fiercewireless.com/special-report/3g-4g-wireless-network-latency-comparing-verizon-at-t-sprint-and-t-mobile-february
[51] *Vehicular Mobility Trace of the city of Cologne, Germany*. Accessed: Apr. 16, 2017. [Online]. Available: http://kolntrace.project.citi-lab.fr/#trace
[52] S. Uppoor, O. Trullols-Cruces, M. Fiore, and J. M. Barcelo-Ordinas, "Generation and analysis of a large-scale urban vehicular mobility dataset," *IEEE Trans. Mobile Comput.*, vol. 13, no. 5, pp. 1061–1075, May 2014.
[53] *OpenStreetMap*. Accessed: Apr. 16, 2017. [Online]. Available: https://www.openstreetmap.org/

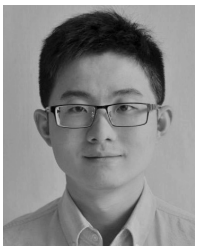

James J. Q. Yu (S'11–M'15) received the B.Eng. and Ph.D. degrees in electrical and electronic engineering from The University of Hong Kong, Hong Kong, in 2011 and 2015, respectively. He is currently a Post-Doctoral Fellow with the Department of Electrical and Electronic Engineering, The University of Hong Kong. His research interests include smart city technologies, power stability analysis, evolutionary algorithm design and analysis, and deep neural network applications.

Albert Y. S. Lam (S'03–M'10–SM'16) received the B.Eng. degree (Hons.) degree in information engineering and the Ph.D. degree in electrical and electronic engineering from The University of Hong Kong (HKU), Hong Kong, in 2005 and 2010, respectively. He was a Post-Doctoral Scholar with the Department of Electrical Engineering and Computer Sciences, University of California at Berkeley, Berkeley, CA, USA, from 2010 to 2012. He is currently a Research Assistant Professor wih the Department of Electrical and Electronic Engineering, HKU. He is a Croucher Research Fellow. His research interests include optimization theory and algorithms, evolutionary computation, smart grid, and smart city.